Pergamon

Int. J. Heat Mass Transfer. Vol. 37, No. 16, pp. 2579–2583, 1994

0017–9310/94 $7.00 + 0.00

TECHNICAL NOTES

Effect of solid conductivity on radiative heat transfer in packed beds

B. P. SINGH and M. KAVIANY†

Department of Mechanical Engineering and Applied Mechanics, The University of Michigan, Ann Arbor, MI 48109, U.S.A.

(*Received* 5 *October* 1993 *and in final form* 24 *March* 1994)

1. INTRODUCTION

THE SOLUTION of the radiative heat transfer problem in porous media has received considerable attention for a number of years (e.g., Vortmeyer [1], Tien and Drolen [2], and Kaviany and Singh [3]). The medium may be considered as a continuum or as a discrete collection of particles, depending on whether the packing lies in the dependent or independent scattering/absorption range. Independent scattering/absorption is said to occur when the interaction between the radiation and a particle is not influenced by the presence of the neighboring particles. Dependent scattering can be divided into a far-field interference influencing the scattering characteristics of the medium and a near-field multiple scattering within a representative elementary volume in which the scattering and absorption characteristics of the particles are affected. Singh and Kaviany [4] show that the limits of independent scattering are a minimum value of porosity ($\varepsilon \simeq 0.95$) and a minimum value of C/λ. The average interparticle clearance distance C for a rhombohedral packing is given by $C/d = 0.905/[(1-\varepsilon)^{1/3}-1]$. Since all practical packed beds and most of the fluidized beds have a porosity lower than this independent limit, the scattering/absorption will generally lie in the dependent range. This implies that the radiative properties of the bed cannot be predicted from the properties of a single particle by the theory of independent scattering/absorption. Then the continuum approach to the packed bed internal radiation becomes difficult unless the properties are determined either experimentally or from discrete models (Singh and Kaviany [5]).

In the dependent range, ray tracing has been successfully used to solve the internal, bed radiative heat transfer (Chen and Tien [6]; Yang *et al.* [7]). Singh and Kaviany [5] have extended this approach to include absorbing and emitting as well as transparent and semi-transparent particles. One limitation of this approach is that the spherical particle diameter has to be much larger than the wavelength of radiation, i.e. the particles must lie in the geometric optic range. However, this is generally satisfied in most packed-bed applications. The second limitation has been that the problem was solved by assuming that the solid conductivity is either very large (as compared with radiant conductivity) or is very small. The difference between the predicted values of the radiant conductivity from these two asymptotes can be quite large (as much as fivefold). This latter limitation provides the motivation for the solution of the generalized problem, i.e. the radiative heat transfer through a packed bed of absorbing–emitting–scattering spheres with an arbitrary solid conductivity. For optically thick media, the concept of radiant conductivity (Vortmeyer [1]) k_r has been used and through this an exchange factor F has been introduced which depends on the particle properties (Tien and Drolen [2]). For opaque particles and for porosites characteristic of packed beds, the use of radiant conductivity is generally valid.

† Author to whom correspondence should be addressed.

In this note, a technique has been developed to model the effect of the solid conductivity on the radiant conductivity in packed beds of spherical particles. The solution is obtained for both diffuse and specular, scattering spheres by combining the Monte Carlo method for the radiation transport and a finite-difference scheme for the temperature distribution within a representative sphere in each layer of a multilayer bed. The results show that the radiant conductivity is strongly influenced by the solid conductivity and the particle emissivity. The computed values for the exchange factor are curve fitted as a function of the dimensionless solid conductivity k_s^* and the particle emissivity ε_r, for a simple-cubic packing. The limits for variation with porosity are discussed. Also, sensitivity studies are carried out which confirm the validity of this technique for computing the radiative conductivity of the bed, as well as establishing the convergence.

2. PROBLEM CONSIDERED

A one-dimensional, plane-parallel medium is used and is rendered in Fig. 1. The problem can be divided into the following two cases. In the case of a cold medium, the medium does not emit in the wavelength of the incident energy. This case is common in optical experiments, where a low-frequency laser irradiation is used and the medium is at room temperature and does not radiate any significant amount of radiation in the wavelength of the incident beam. Also, the experiment of Chen and Churchill [8] can be considered in this class. Methods of solution include the Monte Carlo method (Singh and Kaviany [4]), a simple scaling approach combined with the discrete ordinates method (for opaque spheres, Kaviany [9]), and a more complex variant (DIDOM, Singh and Kaviany [5]) for transparent and semi-transparent spheres.

For the case of a medium emitting in the range of the incident radiation, as considered here, the upper boundary is assumed to be at a temperature T_1 and the lower boundary at a temperature T_2, with both boundaries assumed to be behaving as blackbodies. Consider the two blackbody emissive powers to be related by the relation

$$E_{b_2} = \gamma E_{b_1} \tag{1}$$

where γ varies between 0 and 1. The spheres have a solid conductivity k_s and the matrix has a porosity ε. The objective is to find the radiative heat transfer through the medium.

The low and high conductivity limits of this problem have been explored experimentally (Vortmeyer [1]) and by the Monte Carlo method (Singh and Kaviany [4]). In the low-conductivity asymptote, the rays are considered to be emitted from the same point on the sphere at which they are absorbed. Thus the ray tracing approach may be used successfully. Similarly, the high-conductivity asymptote, i.e. when the solid conductivity is much higher than the radiant conductivity, can be treated with the ray-tracing approach.

NOMENCLATURE

a_i	$i = 1, 2, 3, 4$; constants
C	average interparticle clearance distance [m]
d	particle diameter [m]
E_b	blackbody emissive power [W m^{-2}]
F	exchange factor
k	thermal conductivity [W m^{-1} K^{-1}]
L	bed length [m]
n	number of particle layers
N	number of rays
q	heat flux [W m^{-2}]
s	volumetric heat source [W m^{-3}]
T	temperature [K].

Greek symbols

γ	constant
ε	porosity
ε_r	surface emissivity
λ	wavelength [m]
ρ_r	reflectivity
σ_{SB}	Stefan–Boltzmann constant [W m^{-2} K^{-4}].

Superscript

*	dimensionless.

Subscripts

1, 2	bounding surface 1, 2
b	blackbody or bounding surface
m	mean
r	radiation
s	solid.

An individual sphere is assumed to be isothermal and a ray absorbed by the sphere is given an equal probability of being emitted from anywhere on the sphere surface. This results in an increase in the radiant conductivity (over the low-conductivity case), because the rays absorbed on one side can be emitted from the other side, thus by-passing the radiative resistance.

The general problem, where the solid and the radiant conductivities can have arbitrary magnitudes, has not been explored before. This is the primary objective of this note and the formulation, solution method, and results, are described below.

3. FORMULATION

Consider an absorbing, emitting packed bed of spheres, as shown in Fig. 1. The radiative heat flux, q_r for this one-dimensional, plane geometry is given by (Vortmeyer [1])

$$q_r = \frac{F\sigma_{SB}}{(1+\rho_{r,b})/(1-\rho_{r,b}) + (L/d)}(T_1^4 - T_2^4) \tag{2}$$

where $\rho_{r,b}$ is the bounding surface reflectivity, L is the bed depth, and d is the particle diameter. The radiant conductivity k_r is defined as

$$k_r = 4Fd\sigma_{SB}T_m^3 \tag{3}$$

and

$$F = F(k_s, \varepsilon_r, \varepsilon) \tag{4}$$

where d is the diameter of the sphere, σ_{SB} is the Stefan–Boltzmann constant, T_m is the mean temperature of the bed, and F is the exchange factor and is a function of the given solid conductivity k_s, surface emissivity ε_r, and the porosity of the bed ε. We define a dimensionless solid conductivity k_s^* as

$$k_s^* = \frac{k_s}{4d\sigma_{SB}T_m^3}. \tag{5}$$

The mean bed temperature T_m can be given in terms of the emissive powers of the bounding black surfaces as

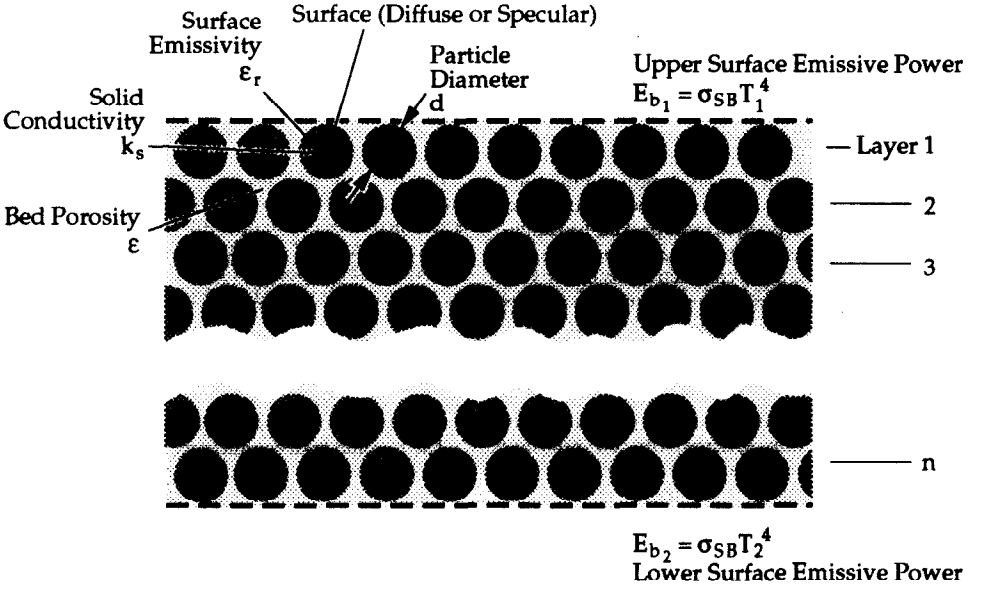

FIG. 1. The plane-parallel geometry considered showing the bounding, emitting surfaces, and layers of particles.

$$T_m^3 = \frac{E_{b_1} - E_{b_2}}{4\sigma_{SB}(T_1 - T_2)}. \quad (6)$$

In this problem $\rho_{r,b} = 0$, so the value of the radiant conductivity can be determined from the heat flux through the bed as

$$k_r = \frac{q_r}{(1 + (L/d))(T_1 - T_2)}. \quad (7)$$

The factor 1 in the denominator is often neglected, because $L \gg d$. Here, in the determination of the exchange factor F, the factor 1 is retained, i.e. once the value of k_r is known, the exchange factor F is calculated from equation (3).

Within the bed, the radiation is treated by combining the ray tracing with the Monte Carlo approach of Singh and Kaviany [5]. The conduction through a sphere is allowed by solving for the temperature distribution in a representative sphere for each particle layer in the bed. The finite-volume approach is used (Patankar [10]) to solve the heat conduction equation

$$k_s \nabla^2 T = \dot{s} \quad (8)$$

where $\dot{s}$ is the source term which is non-zero for the boundary nodes (i.e. surface nodes) and is found from the radiation part of the problem (i.e. the energy absorbed at each location on the surface of the sphere).

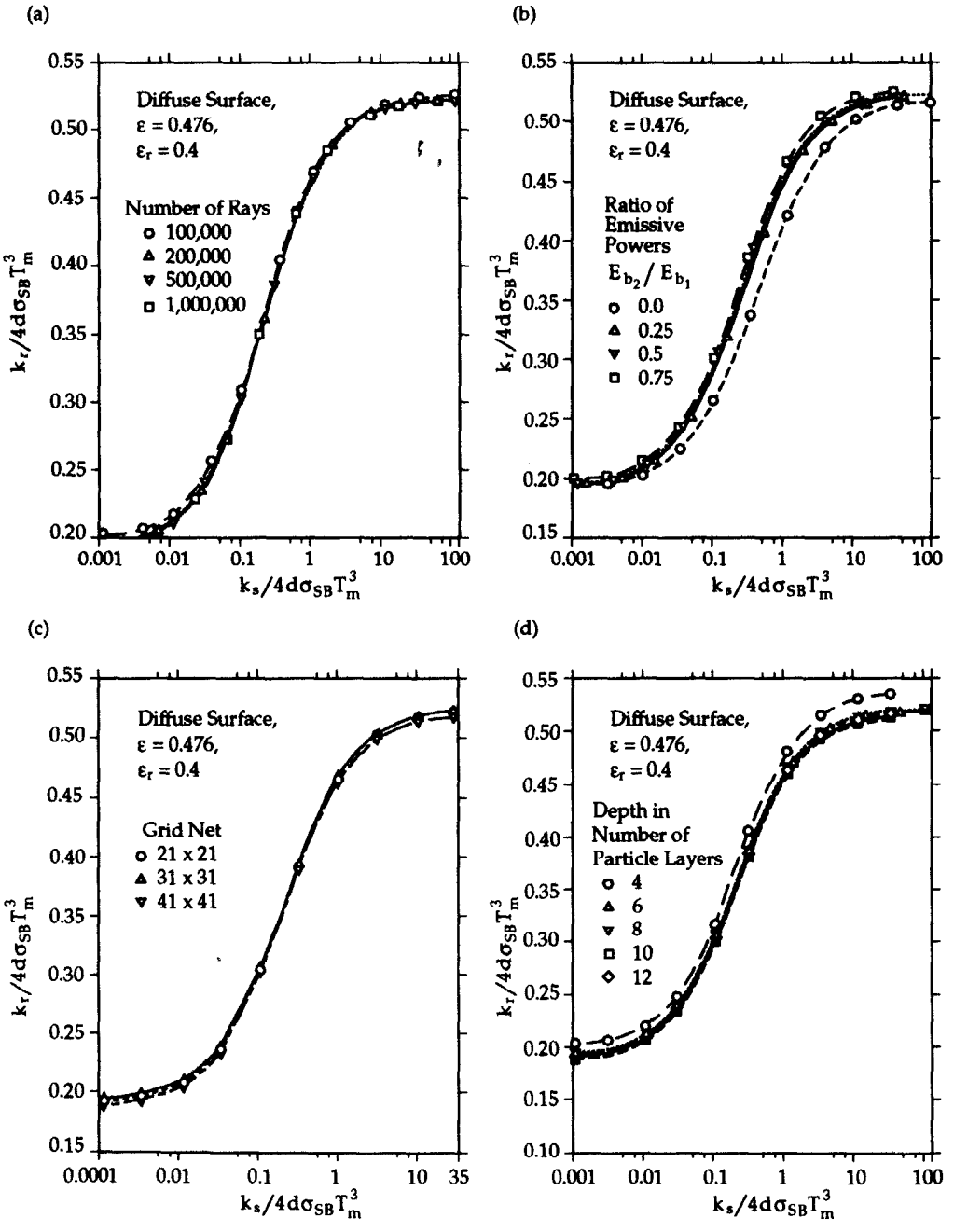

FIG. 2. The results of convergence tests showing the variation of the normalized radiant conductivity with respect to the normalized solid conductivity. (a) Effect of number of rays, (b) effect of ratio of emissive powers, (c) effect of grid-net resolution, and (d) effect of number of particle layers.

4. SOLUTION METHOD

The method of solution combines the Monte Carlo method for a packed bed (Singh and Kaviany [4]) with the finite-volume formulation for a temperature distribution in a sphere. The Monte Carlo method is the same as described in [4]. The important features include the random, horizontal displacement of the particle layers after each individual ray is traced through the bed, in order to simulate a randomly arranged packed bed. Periodic boundary conditions in the horizontal direction are employed in conjunction with a unit cell which includes portions of the four neighboring spheres. The portions included in the unit cell make up one whole sphere and are treated as parts of the same sphere for the solution of the conduction problem. Each sphere (one for every layer in the packed bed) is divided into concentric circles with each band representing the thickness of a finite-volume cell. The upper boundary is allowed to emit a number of rays N_1 and the energy absorbed by each band on each sphere is recorded in a matrix. Similarly, the bottom surface emits a number of rays $N_2 = \gamma N_1$ and the energy absorbed by each band is again recorded. Then, each band on each sphere emits a fixed number of rays and the energy absorbed by every surface is stored in a matrix $E(i_i, j_j, i_0, j_0)$ which represents the fraction of energy emitted by the j_i band on the i sphere that is absorbed by the j_0 band on the i_0 sphere. Also the fraction going to each surface is recorded. Thus the system is divided into a number of surfaces and $E(i_i, j_j, i_0, j_0)$ represents a factor analogous to the view factor in the surface radiation problems. The difference lies in the fact that it takes into account energy from the multiple reflection and the individual spheres actually represent the whole layer, because of the use of periodic boundary conditions.

This procedure results in a significant saving in the computation, since the radiative view factors are stored in the beginning of a run and do not have to be iterated upon along with the conduction solution. Initially, all the spheres are set to the temperature of zero. The bottom and top planes emit a number of rays $N_1 \propto E_{b_1}$ and $N_2 \propto E_{b_2}$. The number of rays absorbed by each band on each sphere is recorded. This represents the boundary conditions for the conduction solution which results in a new temperature distribution in each sphere. Then, in the next radiation iteration, each band on each sphere also emits energy (a function of its temperature recorded in the conduction part) and the energy absorbed by each band is recorded and used as a boundary condition for the next conduction iteration. This procedure is repeated until convergence is reached, i.e. the temperature of each band becomes stable and the net energy transferred from the top surface to the bottom surface no longer changes.

5. RESULTS AND DISCUSSION

Figure 2(a) shows that as the number of rays is increased progressively from 10^5 to 2×10^5 to 5×10^5 to 10^6, a convergence is reached. The number 5×10^5 is used for all the runs considered converged. Changing the number of rays also changes E_{b_1} and E_{b_2}. Note that this independence of E_{b_2} and E_{b_1}, numerically establishes the influence of k_s^* as a parameter (since the same value of F is recorded for different T_1 and T_2 combinations while keeping k_s^* constant). Figure 2(b) shows the convergence with respect to E_{b_2}/E_{b_1}.

Figure 2(c) shows that the number of nodes in the finite-volume conduction solution is increased progressively from 21×21 to 31×31 to 41×41. The results show that a good convergence is found and that the grid net 31×31 is used in all the solutions considered converged. Figure 2(d) shows the effect of the number of layers. A depth of six sphere layers is found to be sufficient to eliminate the boundary effects, thus simulating the bulk properties of a continuous medium. However, eight layers are used in all the runs considered to be converged. Since the properties of the medium (i.e. independent of the boundaries) are determined, the results can be used in any arbitrary medium, as long as each dimension is large compared with the sphere diameter. The results for $\varepsilon = 0.476$ and various values of ε_r and k_s^* have been obtained for both diffusive and specular surfaces. The results are shown in Figs. 3(a) and (b). The results for both surfaces are nearly the same. Both low and high k_s^* asymptotes are present. The low k_s^* asymptotes are reached for $k_s^* < 0.10$ and the high k_s^* asymptote is approached for $k_s^* > 10$. There is a monotonic increase with ε_r, i.e. as absorption increases, the radiant conductivity increases, for high k_s^*.

The results of Figs. 3(a) and (b) have been correlated using

$$F = a_1\varepsilon_r \tan^{-1}\left(a_2\frac{k_s^{*a_3}}{\varepsilon_r}\right)+a_4. \tag{9}$$

The best-fit values of the constants are given in Table 1.

The computer intensive nature of the problem prevented a thorough sweep of the porosity range as an independent variable. However, the effect of the porosity in the high conductivity limit, has been discussed by Singh and Kaviany [3, 4]. For example, by decreasing the porosity from 0.6 to 0.5, the magnitude of F changes from 0.47 to 0.51 for

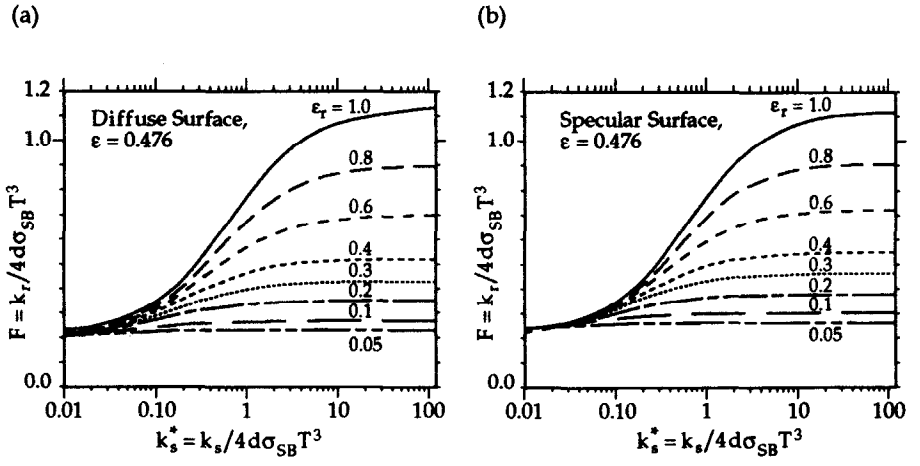

FIG. 3. Variation of the normalized radiant conductivity with respect to the normalized solid conductivity for (a) diffuse particle surfaces, and (b) specular particle surfaces. The results are for $\varepsilon = 0.476$ and for various surface emissivities.

Table 1. Constants in the exchange factor correlation

	Specular	Diffuse
a_1	0.5711	0.5756
a_2	1.4704	1.5353
a_3	0.8237	0.8011
a_4	0.2079	0.1843

$\varepsilon_r = 0.35$ (specular surfaces) and from 0.94 to 0.97 for $\varepsilon_r = 0.85$ (diffuse surfaces). In practical packed beds, the porosity ranges between 0.3 and 0.6 with a value of 0.4 for randomly arranged, loosely packed monosized spheres. Therefore, the sensitivity of the radiant conductivity with respect to the porosity (as compared to other parameters) is not expected to be very significant.

REFERENCES

1. D. Vortmeyer, Radiation in packed solids, *Proceedings of 6th International Heat Transfer Conference*, Toronto, Vol. 6, pp. 525–539 (1978).
2. C.-L. Tien and B. L. Drolen, Thermal radiation in particulate media with dependent and independent scattering, *Ann. Rev. Num. Fluid Mech. Heat Transfer* **1**, 1–32 (1987).
3. M. Kaviany and B. P. Singh, Radiative heat transfer in porous media, *Adv. Heat Transfer* **23**, 133–186 (1993).
4. B. P. Singh and M. Kaviany, Independent theory versus direct simulation of radiative heat transfer in packed beds, *Int. J. Heat Mass Transfer* **34**, 2869–2881 (1991).
5. B. P. Singh and M. Kaviany, Modeling radiative heat transfer in packed beds, *Int. J. Heat Mass Transfer* **35**, 1397–1405 (1992).
6. C. K. Chan and C.-L. Tien, Radiative transfer in packed spheres, *ASME J. Heat Transfer* **96**, 52–58 (1974).
7. Y. S. Yang, J. R. Howell and D. E. Klein, Radiative heat transfer through a randomly packed bed of spheres by the Monte Carlo method, *ASME J. Heat Transfer* **105**, 325–332 (1983).
8. J. C. Chen and S. W. Churchill, Radiant heat transfer in packed beds, *A.I.Ch.E. Jl* **9**, 35–41 (1963).
9. M. Kaviany, *Principles of Heat Transfer in Porous Media*. Springer-Verlag, New York (1991).
10. S. V. Patankar, *Numerical Heat Transfer and Fluid Flow*. Hemisphere, Washington, DC (1980).

Pergamon

Int. J. Heat Mass Transfer. Vol. 37, No. 16, pp. 2583–2587, 1994

0017-9310/94 $7.00+0.00

Visualization of density fields in liquid metals

R. E. POOL and J. N. KOSTER†
Dept. of Aerospace Engineering Sciences, University of Colorado, Boulder, CO 80309-0429, U.S.A.

(*Received* 13 *December* 1993 *and in final form* 4 *March* 1994)

1. INTRODUCTION

THE EXPERIMENTAL study of liquid metal flows is required to better understand the physics of convective fluid flow and heat transfer in materials science applications. Improvement of the quality of electronic solids through control of the convective melt environment requires a thorough grasp of both buoyant and thermocapillary flow mechanisms in low Prandtl number fluids. A large number of convective studies towards this application have been made using high Prandtl number transparent fluids. However, due to the large difference in Prandtl number between transparent fluids and liquid metals, the driving mechanisms for convective flow have a different character. This was presented by, among others, Carpenter and Homsy [1], who showed large differences in surface tension gradients for high Prandtl number fluids vs low Prandtl number fluids. Knowledge of these low Prandtl number flow mechanisms will foster an improved understanding of materials solidification issues.

Because liquid metals are opaque, their study requires the use of unconventional flow analysis techniques. Historically, this has been limited to probing with thermocouples and observations of surface motion [2–4]. Also, highly intrusive electromagnetic techniques were used [5]. A new, non-invasive method of liquid metal flow visualization has recently been developed. The system described here uses real time radioscopy and has been employed with much success to visualize the melting and solidification interfaces [6–8]. The method has now been improved to permit coarse visualization of the density fields in liquid gallium. Analysis of the density fields can yield information concerning the character of the convective flow field as well as the nature of the heat transfer taking place. Real time visualization of the thermal fields is complementary to thermocouple probing because it allows visualization of the entire flow field. In addition, this method is non-intrusive and can be utilized for the visualization of multiple liquid layers where thermocouple techniques would interfere with the interface behavior.

To assess the heat transfer characteristics in a liquid metal it is desirable to have knowledge of the thermal fields within the fluid, especially during convective or unsteady flow. Creating isothermal patterns from convective fluids using the method of holographic interferometry [9] has proven to be useful for determining the character of convective flow. Not only is the temperature field clearly diagrammed, but also

†To whom correspondence should be addressed.